

von MISES TAPERING: A NEW CIRCULAR WINDOWING

H. M. de Oliveira

Federal University of Pernambuco, Statistics Department, Brazil.

<https://orcid.org/0000-0002-6843-0635>

R. J. Cintra

Federal University of Pernambuco, Statistics Department, Brazil.

<https://orcid.org/0000-0002-4579-6757>

ABSTRACT: Discrete and continuous standard windowing are revisited and a new taper is introduced, which is derived from the normal circular distribution by von Mises. Both the continuous-time and the discrete-time windows are considered, and their spectra obtained. A brief comparison with further classical window families is performed in terms of their properties in the spectral domain. These windows can be used in spectral analysis, and in particular, in the design of FIR (finite impulse response) filters as an alternative to the Kaiser window¹.

KEYWORDS: von Mises, tapering function, circular distributions, FIR design.

1 Introduction

Due to the fact that many signals present a quasi-periodic nature, the signal processing techniques developed for real variables in the real line may not be appropriate. For circular data [2], [7], it makes no sense to use the sample mean, usually adopted to the data line as a measure of centrality. Circular measurements occur in many areas [20], such as chronobiology [24], economy [6], geography [3], medical (circadian therapy [25], epidemiology [12]...), geology [41], [34], meteorology [4], acoustic scatter [21] and particularly in signals with some cyclic structure (GPS navigation [27], characterization of oriented textures [5], discrete-time signal processing and over finite fields). Even in political analysis [15]. Probability distributions have been successfully used for several purposes: for example, the beta distribution was used in wavelet construction [9]. Here, the von Mises distribution is used in the design of tapers. Tools such as rose diagram [19] allow rich graphical interpretation. Circular properties for random signals is the main focus here. The uniform distribution of an angle ϕ , circular in the range $[0, 2\pi]$, is given by:

$$f_1(\phi) := \frac{1}{2\pi} \mathbb{I}_{[0, 2\pi]}(\phi), \quad (1)$$

where $\mathbb{I}_A(\cdot)$ is the indicator function of the interval $A \subset \mathbb{R}$. It is denoted by $\phi \sim \mathcal{U}(0, 2\pi)$. Another very relevant circular distribution is the normal circular

¹part of this paper was presented at the SBrT, Brazil, doi 10.14209/SBRT.2018.179

distribution, introduced in 1918 by von Mises, defined in the interval $[0, 2\pi]$ and denoted by $\phi \sim \mathcal{VM}(\phi_0, \beta)$.

$$f_2(\phi) := \frac{1}{2\pi I_0(\beta)} e^{\beta \cos(\phi - \phi_0)}, \quad (2)$$

where $\beta \geq 0$ and $I_0(\cdot)$ is the zero-order modified Bessel function of the First Kind [1] (not to be confused with the indicator function), i.e.

$$I_0(z) := \frac{1}{\pi} \int_0^\pi e^{z \cdot \cos \theta} d\theta = \sum_{n=0}^{+\infty} \frac{(z/2)^{2n}}{n!^2}. \quad (3)$$

This probability density dominates in current analysis of circular data because it

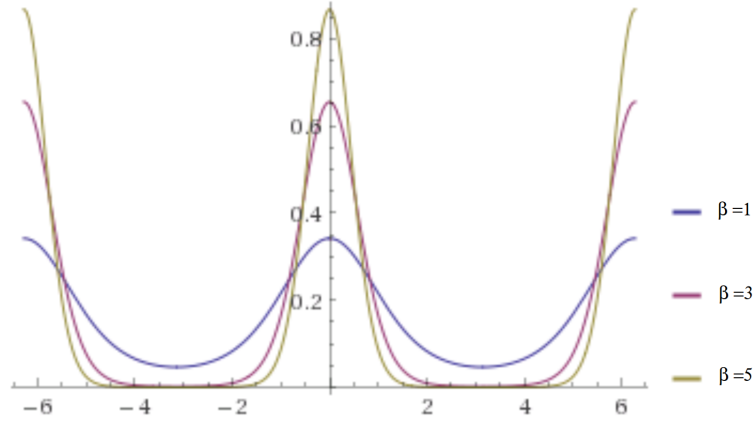


Fig. 1: Periodic extension of the von Mises distribution with zero-mean for several parameter values: $\beta = 1, 3, 5$. Note that the support of the density is confined to $[-\pi, \pi]$.

is flexible with regard to the effect of parameters. In a standard notation,

$$f(x|\mu, \kappa) := \frac{e^{\kappa \cos(x-\mu)}}{2\pi I_0(\kappa)} \cdot \mathbb{I}_{[-\pi, \pi]}. \quad (4)$$

Standardized distribution support is $[-\pi, \pi]$ and the mean, mode and median values are μ . The parameter κ plays a role connected to variance, being $\sigma^2 \approx 1/\kappa$.

$$\mathbb{E}(X) = \mu \text{ and } \mathbb{V}ar(X) = 1 - \frac{I_1(\kappa)}{I_0(\kappa)}.$$

Two limiting behaviors can be observed:

•

$$\lim_{\kappa \rightarrow 0} f(x|\mu, \kappa) = \frac{1}{2\pi} \text{rect}\left(\frac{x}{2\pi}\right), \quad (5)$$

where $\text{rect}(x) := \begin{cases} 1 & \text{if } |x| \leq 1/2 \\ 0 & \text{otherwise.} \end{cases}$ is the gate function, and therefore

$$\lim_{\kappa \rightarrow 0} \mathcal{VM}(\mu, \kappa) \sim \mathcal{U}(-\pi, \pi). \quad (6)$$

•

$$\lim_{\kappa \rightarrow +\infty} f(x|\mu, \kappa) = \frac{1}{\sqrt{2\pi\sigma^2}} e^{-\frac{(x-\mu)^2}{2\sigma^2}}, \quad (7)$$

where $\sigma^2 := 1/\kappa$, and therefore (\mathcal{N} stands for the normal distribution)

$$\lim_{\kappa \rightarrow +\infty} \mathcal{VM}(\mu, \kappa) \sim \mathcal{N}\left(\mu, \frac{1}{\kappa}\right). \quad (8)$$

Hence the reason why this distribution is known as the *circular normal distribution*. The von Mises distribution (\mathcal{VM}) is considered to be a circular distribution having two parameters and it corresponds to as a natural analogue of the the Normal distribution on the real line. Maximum entropy distributions are outstanding probability distributions, because maximizing entropy minimizes the amount of prior information built into the distribution. Furthermore, many physical systems tend to move towards maximal entropy configurations over time. This encompasses distributions such as uniform, normal, exponential, beta...

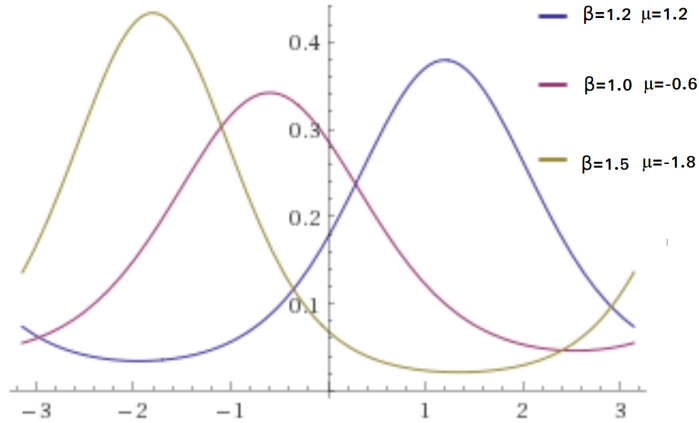


Fig. 2: Circular behavior of the von Mises distribution plotted for different mean values (1.2, -0.6 and -1.8). The cyclical feature of the distribution is shown outside $[-\pi, \pi]$.

The von Mises distribution achieves the maximum entropy for circular data when the first circular moment is specified [20]. The corresponding cumulative distribution function (CDF) is expressed by

$$F_X(x|\mu, \kappa) = \frac{1}{2\pi} \sum_{n=-\infty}^{+\infty} \frac{I_{|n|}(\kappa)}{I_0(\kappa)} (x - |n|) \cdot \text{Sa}(n(x - \mu)), \quad (9)$$

where $\text{Sa}(x) := \sin(x)/x$, $x \neq 0$ is the well-known sample function [26]. Through a simple random variable transformation, the distribution support can be modified to an interval defined between two integers:

$$f_{X_1}(x) := \frac{e^{\beta \cdot \cos(\frac{2\pi}{N}x)}}{NI_0(\beta)}, \text{ circular in } 0 \leq x \leq N. \quad (10)$$

Another closely related continuous distribution (with a minimal - but relevant difference) is:

$$f_{X_2}(x) := \frac{e^{\beta \cdot \cos(\frac{\pi}{N}x)}}{NI_0(\beta)}, \text{ circular in } 0 \leq x \leq N. \quad (11)$$

This distribution has a circular pattern as best illustrated in Figure 2. Decaying pulses for constraining the signal support play a key role in a large number of domains, including: tapers [11], linear networks (filtering [17], inter-symbolic interference control [26]), wavelets [8], time series, Fourier transform spectroscopy [29] ... Digital filters can be characterized by their impulse response $h[n]$ or their transfer function $H(z)$, related by the z -transform [17]:

$$H(z) = \mathcal{Z}(h[n]) := \sum_{n=-\infty}^{+\infty} h[n]z^{-n}. \quad (12)$$

The frequency response can be evaluated by setting $z = e^{j\omega}$, yielding

$$H(e^{j\omega}) = \sum_{n=-\infty}^{+\infty} h[n]e^{-jn\omega}. \quad (13)$$

The window method consists of simply “windowing” a theoretically ideal filter impulse response $h[n]$ by some suitably chosen apodization function $w[n]$, yielding

$$h_w[n] := w[n].h[n], \quad n \in \mathbb{Z}. \quad (14)$$

This results in a truncation of the infinite series referred to in Eqn.(13) (a FIR), i.e.,

$$H_w(e^{j\omega}) = \sum_{n=-N/2}^{N/2} w[n].h[n]e^{-jn\omega}. \quad (15)$$

It can be found in the literature numerous articles dealing with the application of windows in FIR filter designs [38] among others. For example, for the ideal lowpass filter (LPF), the impulse response is $\frac{1}{2} \text{sinc}(\frac{n}{2})$ $n \in \mathbb{Z}$.

2 Tapering: Standard Windows

Here we review some of the continuous and discrete windows (also known as a apodization function) used in signal processing (spectrum analysis [30], [11]), antenna array design [40], characterization of oriented textures [5], image warping and filtering (FIR filter design [37], [17]). Although discrete windows are more common, some studies addressing continuous windows [39], [14], besides their application in short-time Fourier transforms. Among the most frequently used windows, it is worth mentioning: *Rectangular*, *Bartlett*, *cosine-tip*, *Hamming*, *Hanning*, *Blackman*, *Lanczos*, *Kaiser*, *modified Kaiser*, *de la Vallé-Pousin*, *Poisson*, *Saram"aki* [36], *Dolph-Chebyshev*... (non-exhaustive list [33]). Tutorials on the subject are available [13], [33], [16]. The Figure 3 describes the approaches to the standard window, i.e. the rectangular window, considering four cases: 1) continuous non-causal, 2) continuous causal, 3) discrete non-causal, and 4) discrete causal window. These indexes are used in subscribed windows (time and frequency). It is worth revisiting the spectra

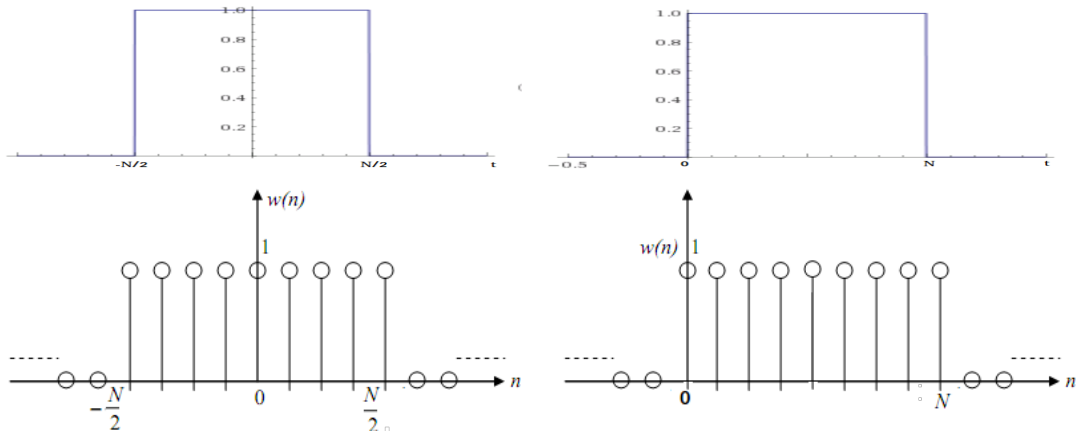


Fig. 3: Rectangular windows with length N (4 types): a) continuous, b) continuous causal, c) discrete, d) discrete causal windows.

of each of these windows.

$$W_{REC;1}(t) = \text{rect}\left(\frac{t}{N}\right), \quad (16a)$$

$$W_{REC;2}(t) = \text{rect}\left(\frac{t - N/2}{N}\right). \quad (16b)$$

In the continuous case, $w_1(t)$ has spectrum given by:

$$W(w) := \mathcal{F}[w(t)] = \int_{-\infty}^{+\infty} w(t)e^{-j\omega t} dt. \quad (17)$$

Indeed $W_{REC;1}(w) = N \cdot \text{Sa}\left(\frac{wN}{2}\right)$. Now the spectrum of $w_{REC;2}(t) = \text{rect}\left(\frac{t - N/2}{N}\right)$ can be evaluated using the time-shift theorem [26], $w(t - t_0) \leftrightarrow W(w) \cdot e^{-j\omega t_0}$, result-

ing in $W_{REC;2}(w) = N \cdot \text{Sa}\left(\frac{wN}{2}\right) e^{-jwN/2}$. The corresponding discrete-time windows are:

$$w_{REC;3}[n] = \begin{cases} 1 & -N/2 \leq n \leq N/2 \\ 0 & \text{otherwise.} \end{cases} \quad (18a)$$

$$w_{REC;4}[n] = \begin{cases} 1 & 0 \leq n \leq N \\ 0 & \text{otherwise.} \end{cases} \quad (18b)$$

In the case of discrete signals (discrete time), the discrete-time Fourier Transform (DTFT) is used:

$$W(e^{j\omega}) := \sum_{n=-\infty}^{+\infty} w[n] \cdot e^{-jn\omega}. \quad (19)$$

The idea behind the use of windowing is to confine the previous summation. For the window $w_{REC;3}[n]$, we have a spectrum:

$$W_{REC;3}(e^{j\omega}) = \sum_{n=-N/2}^{N/2} e^{-jn\omega} = \frac{\sin\left(\frac{N+1}{2}\omega\right)}{\sin(\omega/2)}. \quad (20)$$

This substantially corresponds to the Dirichlet kernel $D(\omega) := \frac{\sin\frac{N+1}{2}\omega}{\sin\frac{\omega}{2}} e^{j\frac{\omega}{2}}$ (or periodic sinc function) [10]. For the causal discrete rectangular $w_{REC;4}[n]$,

$$W_{REC;4}(e^{j\omega}) = \sum_{n=0}^N e^{-jn\omega} = \frac{\sin\left(\frac{N+1}{2}\omega\right)}{\sin(\omega/2)} e^{-j\frac{\omega}{2}N}. \quad (21)$$

A less adopted but appealing notation is the *aliased sinc function*

$$\text{asinc}_M(\omega) := \frac{\text{Sa}(M \cdot \omega/2)}{\text{Sa}(\omega/2)} = \frac{\text{sinc}(Mf)}{\text{sinc}(f)}. \quad (22)$$

For the discrete causal window, the time shift property for the discrete-time Fourier transform can also be used. Several of the windows of interest can be encompassed taking into account the following definition:

$$w_{\alpha;1}(t) := \left\{ \alpha + (1 - \alpha) \cdot \cos\left(\frac{2\pi}{N}t\right) \right\} \cdot \text{rect}\left(\frac{t}{N}\right), \quad (23)$$

The Hanning (raised cosine) window corresponds to $\alpha = 0.5$, whereas the standard Hamming window corresponds to $\alpha = 0.54$ [32]. In the case of a cosine-tip continuous window ($\alpha = 0$), the corresponding window and spectrum are [14]:

$$w_{\alpha=0;1} := \cos\left(\frac{2\pi}{N}t\right) \cdot \text{rect}\left(\frac{t}{N}\right), \quad (24)$$

and therefore,

$$W_{\alpha=0;1}(w) = \frac{N}{2} \cdot \text{Sa} \left(\frac{Nw}{2} - \pi \right) + \frac{N}{2} \cdot \text{Sa} \left(\frac{Nw}{2} + \pi \right). \quad (25)$$

In the discrete case,

$$W_{\alpha=0;4}(e^{j\omega}) = \frac{1}{2} \left[\text{D} \left(\omega - \frac{2\pi}{N} \right) + \text{D} \left(\omega + \frac{2\pi}{N} \right) \right] \cdot e^{-j\omega \frac{N}{2}} \quad (26)$$

We shall denote alternatively by

$$W_{\alpha=0;3}(e^{j\omega}) = \frac{1}{2} \left[\text{asinc}_{N+1} \left(\omega - \frac{2\pi}{N} \right) + \text{asinc}_{N+1} \left(\omega + \frac{2\pi}{N} \right) \right]. \quad (27)$$

For the discrete-time case with arbitrary α (Eqn.(23)), we have the following linear combination of spectra:

$$W_{\alpha;3}(e^{j\omega}) = \alpha \cdot W_{\alpha=1;3}(e^{j\omega}) + (1 - \alpha) \cdot W_{\alpha=0;3}(e^{j\omega}). \quad (28)$$

The Kaiser window in continuous variable is defined by (non-causal window centered on the origin, and its corresponding causal version)

$$w_{KAI;1}(t) := \frac{I_0 \left(\beta \sqrt{1 - \left(\frac{t}{N/2} \right)^2} \right)}{I_0(\beta)} \cdot \text{rect} \left(\frac{t}{N} \right), \quad (29a)$$

$$w_{KAI;2}(t) := \frac{I_0 \left(\beta \sqrt{1 - \left(\frac{t-N/2}{N/2} \right)^2} \right)}{I_0(\beta)} \cdot \text{rect} \left(\frac{t - N/2}{N} \right). \quad (29b)$$

In the case of discrete versions (those that are used in filter designs), the corresponding versions are [23]: a) non causal and b) causal, respectively.

$$w_{KAI;3}[n] := \begin{cases} \frac{I_0 \left(\beta \sqrt{1 - \left(\frac{n}{N/2} \right)^2} \right)}{I_0(\beta)} & 0 \leq n \leq N \\ 0 & \text{otherwise.} \end{cases} \quad (30a)$$

$$w_{KAI;4}[n] := \begin{cases} \frac{I_0 \left(\beta \sqrt{1 - \left(\frac{n-N/2}{N/2} \right)^2} \right)}{I_0(\beta)} & -N/2 \leq n \leq N/2 \\ 0 & \text{otherwise.} \end{cases} \quad (30b)$$

The spectrum of discrete Kaiser windows can be evaluated resulting in [23]:

$$W_{KAI;3}(e^{j\omega}) = \frac{N}{I_0(\beta)} \text{Sa} \left(\sqrt{\left(\frac{N\omega}{2}\right)^2 - \beta^2} \right). \quad (31)$$

3 Introducing the Circular Normal Window

The proposal here is to use a window (support length N) with shape related to

$$W(t) = K \cdot \frac{e^{\beta \cdot \cos(\frac{\pi}{N}t)}}{I_0(\beta)} \cdot \text{rect} \left(\frac{t}{N} \right). \quad (32)$$

The value of the constant K can be set so that, as in the other classic windows, $w(0) = 1$. Thus, for continuous cases (both not causal and causal), one has:

$$W_{CIR;1}(t) = \frac{e^{\beta \cdot \cos(\frac{\pi}{N}t)}}{e^\beta} \cdot \text{rect} \left(\frac{t}{N} \right), \quad (33a)$$

$$W_{CIR;2}(t) = \frac{e^{\beta \cdot \cos(\frac{\pi}{N}t)}}{e^\beta} \cdot \text{rect} \left(\frac{t - N/2}{N} \right), \quad (33b)$$

For the discrete circular windows in time, consider the definitions:

$$W_{CIR;3}[n] = e^{\beta \cdot [\cos(\frac{n\pi}{N}) - 1]}, \quad |n| \leq N/2. \quad (34a)$$

$$W_{CIR;4}[n] = e^{\beta \cdot [\cos(\frac{\pi}{N}(n - \frac{N}{2})) - 1]}, \quad 0 \leq n \leq N. \quad (34b)$$

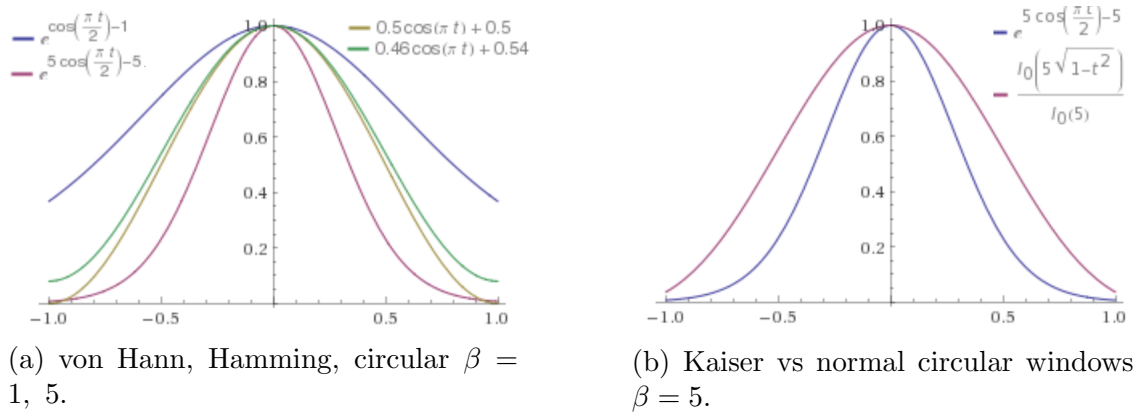


Fig. 4: Shape comparison of different normalized windows for support: $[-1, 1]$.

4 Spectrum of the Normal Circular Window: the Continuous Case

In order to evaluate the spectrum of the continuous window introduced in the previous section, we use Eqn. (17),

$$W_{CIR;1}(w) = \int_{-N/2}^{N/2} e^{\beta \cdot [\cos(\frac{\pi}{N}t) - 1]} e^{-jwt} dt \quad (35)$$

The interest function involved in defining the window is $\cos(\frac{\pi}{N}t)$, with period $2N$, sketched below in $[-N, N]$. The rectangular term included in the window is responsible for cutting the window, confining it in the range $[-N/2, N/2]$ as viewed in Figure 5. MacLaurin's serial development of $e^{\beta \cdot [\cos(\frac{\pi}{N}t)]}$ gives:

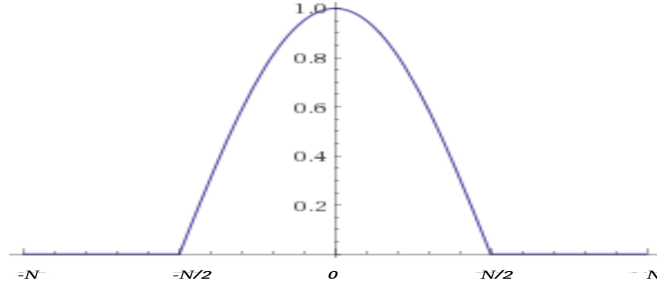


Fig. 5: Normalized cosine exponent of the exponential function in von Mises window: the (entire) cosine $\cos(\pi t/N)$ is periodic in $[-N, N]$, but the support is confined within $[-N/2, N/2]$ due to the rectangular pulse.

$$e^{\beta \cdot [\cos(\frac{\pi}{N}t)]} = \sum_{n=-\infty}^{+\infty} I_{|n|}(\beta) \cos\left(\frac{n\pi}{N}t\right). \quad (36)$$

Thus, one obtains:

$$W_{CIR;1}(w) = e^{-\beta} \sum_{n=-\infty}^{+\infty} I_{|n|}(\beta) \cdot \mathcal{F} \left(\cos\left(\frac{n\pi}{N}t\right) \cdot \text{rect}\left(\frac{t}{N}\right) \right). \quad (37)$$

From the property of the convolution ([26]), the spectrum sought is:

$$W_{CIR;1}(w) = \frac{1}{2\pi} e^{-\beta} \sum_{n=-\infty}^{+\infty} I_{|n|}(\beta) \cdot \mathcal{F} \left(\cos\left(\frac{n\pi}{N}t\right) \right) * \mathcal{F} \left(\text{rect}\left(\frac{t}{N}\right) \right). \quad (38)$$

By evaluating the internal terms of the summation, one come easily to

$$\frac{N}{2\pi} \cdot \pi \cdot \left\{ \delta\left(w - \frac{n\pi}{N}\right) + \delta\left(w + \frac{n\pi}{N}\right) \right\} * \text{Sa}\left(\frac{wN}{2}\right), \quad (39)$$

where $\delta(\cdot)$ is the Dirac impulse [26] and finally,

$$W_{CIR;1}(w) = \frac{N}{2} \cdot e^{-\beta} \cdot \sum_{n=-\infty}^{\infty} I_{|n|}(\beta) \left\{ \text{Sa} \frac{N}{2} \left(w - \frac{n\pi}{N} \right) + \text{Sa} \frac{N}{2} \left(w + \frac{n\pi}{N} \right) \right\}, \quad (40)$$

so,

$$W_{CIR;1}(w) = N \cdot e^{-\beta} \cdot \sum_{n=-\infty}^{\infty} I_{|n|}(\beta) \left\{ \text{Sa} \left(\frac{Nw}{2} - \frac{n\pi}{2} \right) \right\}. \quad (41)$$

This expression is as if a series of reconstitution (with coefficients c_n) of the type:

$$\sum_{n=-\infty}^{+\infty} c_n \cdot \text{Sa} \left(\frac{Nw}{2} - \frac{n\pi}{2} \right).$$

Let us now apply the Shannon-Nyquist-Koteln'kov sampling theorem in the frequency domain, for time-limited signals ([22], <http://ict.open.ac.uk/classics>).

$$F(w) = \frac{w_s t_m}{\pi} \sum_{n=-\infty}^{+\infty} F(nw_s) \text{Sa}(wt_m - nt_m w_s). \quad (42)$$

The rate w_s must comply with the restriction $w_s \leq \pi/t_m$, and the choice made is $w_s = \pi/2t_m$, so that the previous equation is:

$$F(w) = \frac{1}{2} \sum_{n=-\infty}^{+\infty} F\left(\frac{n\pi}{2t_m}\right) \text{Sa} \left(wt_m - \frac{n\pi}{2} \right). \quad (43)$$

Now let us choose the duration t_m to be $t_m := N/2$ (Figure 5).

$$F(w) = \frac{1}{2} \sum_{n=-\infty}^{+\infty} F\left(\frac{n\pi}{N}\right) \text{Sa} \left(\frac{w \cdot N}{2} - \frac{n\pi}{2} \right). \quad (44)$$

This is a variation of the cardinal Whittaker-Shannon series [28].

$$F(w) = \sum_{n=-\infty}^{+\infty} F\left(\frac{2\pi n}{N}\right) \cdot \text{Sa} \left(\frac{wN}{2} - n\pi \right). \quad (45)$$

Observing the series described in Eqn. (41), it is seen that the signal corresponds to a continuous signal defined by samples such that $F\left(\frac{n\pi}{N}\right) = 2I_{|n|}(\beta)$ and

$$F(w) = 2I_{\left|\frac{Nw}{\pi}\right|}(\beta). \quad (46)$$

And the spectrum is given by:

$$W_{CIR;1}(w) = \frac{2NI_{|\frac{Nw}{\pi}|}(\beta)}{e^\beta}. \quad (47)$$

In the case of the causal window, $w_{CIR;1}(t)$, the application of the time-shift theorem provides the spectrum:

$$W_{CIR;2}(w) = \frac{2NI_{\frac{N}{\pi}|w|}(\beta)}{e^\beta} \cdot e^{-jw\frac{N}{2}}. \quad (48)$$

It is worth remembering that the ν argument of the $I_\nu(z)$ is a real number [1].

5 Spectrum of the Normal Circular Window: the Discrete Case

The spectrum of $w_{CIR;3}[n]$ (non causal signal) is evaluated by the discrete-time Fourier transform (Eqn. (19)),

$$W_{CIR;3}(e^{j\omega}) = \sum_{n=-N/2}^{N/2} \frac{e^{\beta \cdot \cos(\frac{\pi n}{N})}}{e^\beta} \cdot e^{-j\omega n}. \quad (49)$$

It is proposed to use the infinite series

$$e^{\beta \cos \theta} = \sum_{k=-\infty}^{+\infty} I_{|k|}(\beta) \cdot \cos k\theta. \quad (50)$$

yielding:

$$W_{CIR;3}(e^{j\omega}) = e^{-\beta} \sum_{k=-\infty}^{+\infty} I_{|k|}(\beta) \cdot \sum_{n=-N/2}^{N/2} \cos\left(n\frac{\pi k}{N}\right) e^{j\omega n}. \quad (51)$$

Now, using the DTFT of a pulse $\cos\left(n\frac{k\pi}{N}\right)$ confined within $|n| \leq N/2$, we take the spectrum of the cosine-tip window with parameter $\alpha = 0$.

$$w_{\alpha=0;3}[n] := \cos\frac{2\pi}{N}n \quad -N/2 \leq n \leq N/2,$$

whose spectrum is given in Eqn. (27). By adjusting properly, one gets

$$W_{CIR;3}(e^{j\omega}) = \sum_{k=-\infty}^{+\infty} \frac{I_{|k|}(\beta)}{2e^\beta} \left[\text{asinc}_{N+1}\left(\omega - \frac{k\pi}{N}\right) + \text{asinc}_{N+1}\left(\omega + \frac{k\pi}{N}\right) \right], \quad (52)$$

or, finally

$$W_{CIR;3}(e^{j\omega}) = \sum_{k=-\infty}^{\infty} \frac{I_{|k|}(\beta)}{e^{\beta}} \cdot \text{asinc}_{N+1}\left(\omega - \frac{k\pi}{N}\right). \quad (53)$$

For fixed β , as $|k|$ increases, the coefficients $I_{|k|}(\beta)/e^{\beta}$ are bounded by $1/\sqrt{2\pi\beta}$ and

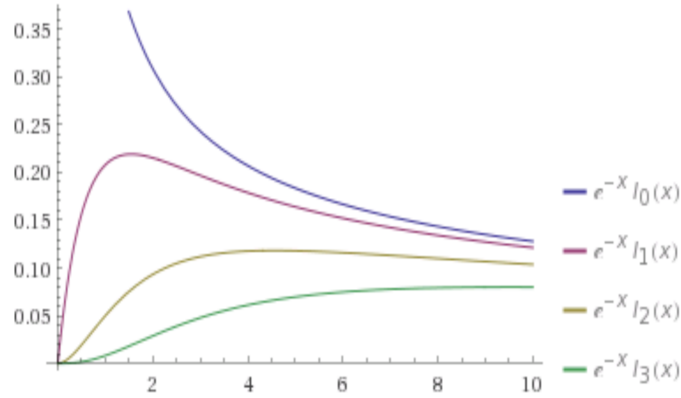


Fig. 6: Asymptotic behavior of the coefficients $I_{|k|}(\beta)/e^{\beta}$

decrease monotonically as observed in Figure 6. Now it is possible to go further and evaluate the taper performances according to [16], [30], [14].

6 Conclusions

The closeness to the normal distribution and the fact that it is associated with a shape linked to the maximum entropy for circular data suggests interesting properties to be explored in later investigations. It is expected that the windowing by von Mises' taper can improve spectral evaluation in cases with circular symmetry.

References

- [1] Abramowitz, M., and I.A. Stegun. *Handbook of Mathematical Functions with Formulas, Graphs, and Mathematical Tables*. Vol.9. Dover, New York, 1972. http://people.math.sfu.ca/~cbm/aands/abramowitz_and_stegun.pdf.
- [2] Berens, P. CircStat: a MATLAB toolbox for circular statistics. *J Stat Softw* 31.10: 1-21, 2009. doi: 10.18637/jss.v031.i10
- [3] Clark, W.A.V., and J.E. Burt. The impact of workplace on residential relocation. *Annals of the Association of American Geographers* 70.1:59-66, 1980 doi: 10.1111/j.1467-8306.1980.tb01297.x
- [4] Coles, S.G., and D. Walshaw. Directional modelling of extreme wind speeds. *Applied Statistics*, 139-157, 1994 doi: 10.2307/2986118.

- [5] Da Costa, J.-P, et al. Unsupervised segmentation based on Von Mises circular distributions for orientation estimation in textured images. *Journal of Electronic Imaging* 21.2: 021102-1, 2012. doi: 10.1117/1.JEI.21.2.021102.
- [6] Dalkir, M. Revisiting stock market index correlations. *Finance Research Letters* 6.1: 23-33, 2009 doi: 10.1016/j.frl.2008.11.004.
- [7] Damien, P., and S. Walker. A full Bayesian analysis of circular data using the von Mises distribution. *Canadian Journal of Statistics* 27.2: 291-298, 1999. doi: 10.2307/3315639.
- [8] de Oliveira, H.M., L.R. Soares, and T.H. Falk. A Family of Wavelets and a New Orthogonal Multiresolution Analysis Based on the Nyquist Criterion, *Journal of Communication and Information Systems* 18.1: 69-76, 2003. doi: 10.14209/jcis.2003.8.
- [9] de Oliveira, H.M. and G.A.A. Araujo. Compactly Supported One-cyclic Wavelets Derived from Beta Distributions, *Journal of Communication and Information Systems*, vol.20, n.3, pp.27-33, 2005. doi: 10.14209/jcis.2005.17
- [10] Dirichlet, P.G.L. Sur la convergence des séries trigonometriques qui servent à représenter une fonction arbitraire entre des limites données *J. für Math.*, 4: 157–169, 1829. <https://arxiv.org/abs/0806.1294v1>
- [11] Durrani, T.S., and J.M. Nightingale. Data windows for digital spectral analysis. *Proceedings of the Institution of Electrical Engineers*. Vol. 119. No. 3. IET Digital Library, 1972. doi: 10.1049/piee.1972.0080
- [12] Gao, F., et al. On the application of the von Mises distribution and angular regression methods to investigate the seasonality of disease onset. *Statistics in medicine* 25.9: 1593-1618, 2006. doi: 10.1002/sim.2463.
- [13] Gautam, J.K., A. Kumar, and R. Saxena. Windows: A tool in signal processing. *IETE Technical Review* 12.3: 217-226, 1995. doi: 10.1080/02564602.1995.11416530.
- [14] Geçkinli, N., and D. Yavuz. Some novel windows and a concise tutorial comparison of window families. *IEEE Transactions on Acoustics, Speech, and Signal Processing* 26.6: 501-507, 1978. doi: 10.1109/TASSP.1978.1163153
- [15] Gill, J. and D. Hangartner. Circular data in political science and how to handle it, *Political Analysis* 18(3): 316-336, 2010. doi: 10.1093/pan/mpq009
- [16] Harris, F.J. On the use of Windows for harmonic analysis with the Discrete Fourier Transform. *Proceedings of the IEEE* 66(1): 51-83. 1978. doi: 10.1109/PROC.1978.10837.

- [17] Hayes, M.H. *Schaum's Outline of Theory and Problems of Digital Signal Processing*, 1999, McGraw-Hill Companies [Chapter 9]
- [18] Hill, G.W. Algorithm 518: Incomplete Bessel function I_0 . The Von Mises Distribution [S14]. *ACM Transactions on Mathematical Software (TOMS)* 3.3: 279-284, 1977. doi: 10.1145/355744.355753
- [19] Izbicki, R. *Análise de Dados Circulares*, Trabalho IC, Instituto de Matemática e Estatística da Universidade de São Paulo-IME-USP, 29p., 2008.
- [20] Jammalamadaka, S. R., and A. Sengupta. *Topics in circular statistics*. Vol. 5. World Scientific, 2001.
- [21] Jenison, R. L., and K. Fissell. A comparison of the von Mises and Gaussian basis functions for approximating spherical acoustic scatter. *IEEE transactions on neural networks* Vol 6.5: 1284-1287, 1995. doi: 10.1109/72.410375.
- [22] Jerri, A.J. The Shannon sampling theorem— Its various extensions and applications: A tutorial review. *Proceedings of the IEEE* 65.11 (1977): 1565-1596. doi: 10.1109/PROC.1977.10771.
- [23] Kaiser, J., and R. Schafer. On the use of the I_0 -sinh window for spectrum analysis. *IEEE Transactions on Acoustics, Speech, and Signal Processing* 28.1: 105-107, 1980. doi: 10.1109/TASSP.1980.1163349.
- [24] Karp-Boss, L., E. Boss, and P.A. Jumars. Motion of dinoflagellates in a simple shear flow. *Limnology and oceanography* 45.7: 1594-1602, 2000 doi: 10.4319/lo.2000.45.7.1594.
- [25] Kirst, C., M. Timme, and D. Battaglia. Dynamic information routing in complex networks. *Nature communications* 7, 2016. doi: 10.1038/ncomms11061.
- [26] Lathi, B.P. and Z. Ding. *Modern Digital and Analog Communication Systems*, 4th Ed, Oxford University press, 2008.
- [27] Luo, X., M. Mayer, and B. Heck. On the probability distribution of GNSS carrier phase observations. *GPS solutions* 15.4: 369-379, 2011 doi: 10.1007/s10291-010-0196-2
- [28] Marks II, R. *Introduction to Shannon sampling and interpolation theory*. Springer Science & Business Media, 2012.
- [29] Naylor, D.A., and M.K. Tahic. Apodizing functions for Fourier transform spectroscopy. *Journal of the Optical Society of America A* 24.11: 3644-3648, 2007. doi: 10.1364/JOSAA.24.003644

- [30] Nuttall, A.H. Some windows with very good sidelobe behavior. *IEEE Transactions on Acoustics, Speech, and Signal Processing* 29 (1): 84–91. 1981. doi: 10.1109/TASSP.1981.1163506
- [31] Parker, K.J. Correspondence: apodization and windowing functions. *IEEE transactions on ultrasonics, ferroelectrics, and frequency control* 60.6: 1263-1271, 2013. doi: 10.1109/TUFFFC.2013.2691.
- [32] Podder, P. et al. Comparative performance analysis of Hamming, Hanning and Blackman window. *International Journal of Computer Applications* 96.18, 2014. doi: 10.5120/16891-6927
- [33] Poularikas A.D. *Windows: The Handbook of Formulas and Tables for Signal Processing*. Ed. A.D. Poularikas, Boca Raton: CRC Press LLC, 1999.
- [34] Prévot, M., and P. Camps. Absence of preferred longitude sectors for poles from volcanic records of geomagnetic reversals. *Nature* 366.6450:53-57,1993 doi: 10.1038/366053a0.
- [35] Samad, A. A novel window function yielding suppressed mainlobe width and minimum sidelobe peak <https://10.5121/ijcseit.2012.220> <https://arxiv.org/abs/1205.1618>
- [36] Saramaki, T. A class of window functions with nearly minimum sidelobe energy for designing FIR filters, 1989, *IEEE International Symposium on Circuits and Systems*, 1989. doi: 10.1109/ISCAS.1989.100365
- [37] Shayesteh, M.G. and M. Mottaghi-Kashtiban. An efficient window function for design of FIR filters using IIR filters. EUROCON 2009. IEEE, 2009. doi: 10.1109/EURCON.2009.5167830
- [38] Smith III, J.O. *Spectral Audio Signal Processing*. W3K publishing, 2011. <https://ccrma.stanford.edu/~jos/sasp/>
- [39] Theußl, T., H. Hauser, and E. Gröller. Mastering windows: improving reconstruction. *Proceedings of the 2000 IEEE symposium on Volume visualization*. ACM, 2000. doi: 10.1109/VV.2000.10002
- [40] Van Veen B.D. and K. Buckley. Beamforming: a versatile approach to spatial filtering, *IEEE ASSP Magazine*, April: 4-24, 1988 doi: 10.1109/53.665.
- [41] Watson, G.S. The statistics of orientation data. *The Journal of Geology* 74.5, Part 2: 786-797, 1966 doi: 10.1086/627211.